ELSEVIER

Journal of Food Engineering 34 (1997) 109–122

PII: S0260-8774(97)00098-8 0260-8774/98 $19.00+0.00

Drying Characteristics of Hemispherical Solids

J. Bon,[a] S. Simal,[b] C. Rosselló[b] & A. Mulet[a]*

[a]Food Technology Department, University Politècnica of València, Cno Vera, s/n, 46071 València, Spain
[b]Department of Chemistry, University of Illes Balears, Ctra Valldemossa, 07071 Palma de Mallorca, Spain

(Received 18 June 1997; accepted 10 November 1997)

ABSTRACT

A diffusional model has been proposed to simulate the drying curves of hemispherical bodies. The equation representative of the mass transfer in terms of Fick's law for a hemispherical shaped body has been solved by separation of variables. By using this solution and the optimization capabilities included in Microsoft Excel 5·0^{TM} spreadsheet, an effective diffusivity coefficient was identified for potatoes at different air drying temperatures (30, 50, 70 and 90°C). Effective diffusivity varied with air drying temperature according to the Arrhenius equation. Experimental data obtained using the same and different experimental conditions of air drying temperature (from 30 to 90°C) and sample size (hemispheres with radius from 0·0128 to 0·0230 m) could be predicted by using the proposed model (%var = 99·7%). The importance of taking into account the real geometry of the solid was evaluated by using the solution for a spherical shaped body. The model developed for a sphere provided less satisfactory results in the simulation of the drying experiments mentioned (%var = 96·6%).

NOMENCLATURE

D_{eff}	Effective diffusivity ($m^2\,s^{-1}$)
D_o	Pre-exponential factor Arrhenius equation ($m^2\,s^{-1}$)
E_a	Activation energy ($J\,mol^{-1}$)
$J_n(x)$	Bessel function of the first kind of order n
$P_n(x)$	Legendre polynomial of the first kind of degree n
r	r axis distance (m)

*To whom all correspondence should be addressed.

R	Hemisphere radius (m)
R	Gas constant (J mol^{-1} K)
S_{yx}	Standard deviation (estimation) (kg water per kg dm)^2
S_y	Standard deviation (sample) (kg water per kg dm)^2
t	Time (s)
T	Drying air temperature (°C)
V	Volume of the hemisphere ($2/3\pi R^3$) (m^3)
W	Local moisture content (kg water per kg dm)
W_c	Critical moisture content (kg water per kg dm)
W_e	Equilibrium moisture content (kg water per kg dm)
W_o	Initial moisture content (kg water per kg dm)
Ψ	Local dimensionless moisture content
Ψ_M	Average dimensionless moisture content
%var	Percentage of explained variance

INTRODUCTION

Drying processes are of major importance in both chemical and engineering industries (Aminabhavi & Phyade, 1995). A full understanding of these types of processes is required to determine optimal operation conditions (Zakhia *et al.*, 1995). In numerous industrial applications, simple but accurate models describing the phenomena involved are also required.

A complete drying profile consists of two stages: the first stage of drying, a constant-rate period; and a falling-rate period. Nevertheless, not all solid bodies follow this pattern. In most applications the dominating stage is the falling-rate period (Dincer & Dost, 1995). It is frequently agreed that the mechanism of moisture movement within a hygroscopic solid could be represented by a diffusion phenomenon as stated by Fick's law.

The effective diffusivity estimated from drying data, represents an overall mass transport property of water in the material, which may include liquid diffusion, vapor diffusion, hydrodynamic flow and other possible mass transfer mechanisms (Karathanos *et al.*, 1990).

Analytical solutions of the equations representative of mass transfer in terms of Fick's law have been reported for geometrical shapes such as spheres, infinite slabs, infinite cylinders, parallelepipeds and finite cylinders (Karathanos *et al.*, 1990; Jaros *et al.*, 1992; Zogzas *et al.*, 1994; Simal *et al.*, 1996a). Nevertheless, several food products present hemispherical shape, for example, mushrooms, halved apricots, coffee grains, some kinds of bread or are frequently modeled in this geometry, halved melons and potato, etc. However, there is no information in the literature regarding the use of this method to solve the mass transfer equation in a hemisphere. More complex models have been used based on finite element techniques (Vanegas & Marinos-Kouris, 1991). A hemispherical shape was considered for the drying of cauliflower florets (García-Reverter *et al.*, 1996), the model being solved by using numerical techniques.

When a model is proposed, comparison of predicted drying curves with experimental curves constitutes a test of the model goodness. If model coefficients were determined directly from experimental data, agreement between the predicted and the observed values does not always validate the model theory. The theoretical basis of the model is indirectly supported when predictions employing these coefficients happened to be good over a broad range of conditions by using data which were not considered for model building (Waananen *et al.*, 1993).

The aim of this study was to propose and evaluate a mathematical model to simulate the drying curves of hemispherical solids. Moreover, the importance of taking into account the real shape of the solid being dried is also evaluated. For the experimental testing drying of potato hemispheres was chosen.

Mathematical model

Assuming that the heat transfer coefficient is high, internal mass transfer resistance prevails and moisture transfer rate in a hemispherical shaped body is only a function of a constant effective diffusivity, then the local moisture content can be calculated through Fick's law combined with the microscopic mass balance. The differential equation obtained for a hemispherical shape is as follows (García-Reverter *et al.*, 1996) where r and α are defined as shown in Fig. 1.

$$D_{\mathrm{eff}}\left[\frac{1}{r^2}\frac{\partial}{\partial r}\left(r^2\frac{\partial\Psi}{\partial r}\right)+\frac{1}{r^2\sin\alpha}\frac{\partial}{\partial\alpha}\left(\sin\alpha\frac{\partial\Psi}{\partial\alpha}\right)\right]=\frac{\partial\Psi}{\partial t} \tag{1}$$

where Ψ is a function of r, α and t being defined by:

$$\Psi=\frac{W-W_{\mathrm{e}}}{W_{\mathrm{c}}-W_{\mathrm{e}}} \tag{2}$$

In order to solve this partial differential equation the following should be assumed:

(1) the initial moisture content is uniform throughout the solid (Karathanos *et al.*, 1990);
(2) the surface moisture of the solid is at equilibrium with the drying air for the time considered (Fusco *et al.*, 1991); and
(3) the shape of the solid remains constant during the period considered (Tolaba *et al.*, 1989).

From these considerations the corresponding initial and boundary conditions at time t can be defined as follows:

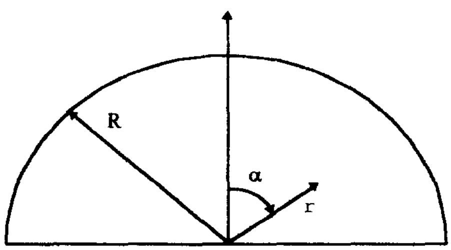

Fig. 1. Definition of r and α in a hemispherical shape.

Initial condition

$$t=0 \quad \Psi=1 \tag{3}$$

Boundary conditions

$$r=\mathrm{R} \quad \Psi=0 \tag{4}$$

$$r=0 \quad \Psi=0 \tag{5}$$

$$\alpha=\frac{\pi}{2} \quad \Psi=0 \tag{6}$$

$$\alpha=0 \quad \frac{\mathrm{d}\Psi}{\mathrm{d}t}=0 \tag{7}$$

By using the separation of variables method (Arpaci, 1966), the following expression was obtained for the moisture profile in the solid:

$$\Psi=\sum_{n=0}^{\infty}\left(\sum_{m=1}^{\infty} a_{nm}\frac{J_{C_n}(\beta_{nm}r)}{r^{\frac{1}{2}}}\exp(-D_{\mathrm{eff}}\beta_{\mathrm{nm}}^{2}\mathrm{t})\right)P_{2n+1}(\cos\alpha) \tag{8}$$

The coefficient a_{nm} is computed by using:

$$a_{nm}=\frac{[8n+6]\int_0^1 P_{2n+1}(x)\mathrm{d}x\int_0^{\mathrm{R}} r^{\frac{3}{2}}J_{C_n}(\beta_{\mathrm{nm}}\mathrm{r})\mathrm{dr}}{\mathrm{R}^2\mathrm{J}^2_{\mathrm{C}_n+1}(\beta_{\mathrm{nm}}\mathrm{R})} \tag{9}$$

In this equation the coefficients $(\beta_{nm}\mathrm{R})$ are the roots of eqn (10)

$$J_{C_n}(\beta_{\mathrm{nm}}\mathrm{R})=0 \tag{10}$$

The eigenvalues, λ_n, are readily obtained using:

$$\lambda_n^2=2(n+1)(2n+1) \tag{11}$$

The eigenvalues determine the order of the Bessel function according to:

$$C_n=\sqrt{\lambda_n^2+\tfrac{1}{4}} \tag{12}$$

In order to fit or predict a drying curve, it was necessary to determine an equation representative of the average moisture content. Therefore, the calculated average moisture could be compared with the corresponding experimental results. This magnitude was expressed as follows:

$$\Psi_{\mathrm{M}}V=\int_V \Psi\,\mathrm{d}V \tag{13}$$

where $\mathrm{d}V$ is the differential volume ($2\pi r^2\sin\alpha\,\mathrm{d}r\,\mathrm{d}\alpha$).

After integration, eqn (14) was obtained, allowing the calculation of the average dimensionless moisture in a hemispherical body as a function of time.

$$\Psi_{\mathrm{M}}=\sum_{n=0}^{\infty}\sum_{m=1}^{\infty} b_{nm}\exp(-\mathrm{D}_{\mathrm{eff}}\beta_{\mathrm{nm}}^2\mathrm{t}) \tag{14}$$

where the coefficient b_{nm} is computed according to:

$$b_{nm} = \frac{(24n+18)\left[\int_0^1 P_{2n+1}(x)\mathrm{d}x \int_0^R r^{\frac{3}{2}} J_{C_n}(\beta_{\mathrm{nm}}\mathrm{r})\mathrm{dr}\right]^2}{\mathrm{R}^5 \mathrm{J}^2_{\mathrm{C}_n+1}(\beta_{\mathrm{nm}}\mathrm{R})} \tag{15}$$

For comparison purposes a dimensionless distance $\delta = r/\mathrm{R}$ can be used. In eqn (15), there is no difficulty in introducing that variable.

Computing the coefficients a_{nm} or b_{nm} is a tedious task since they involve different Legendre polynomials and Bessel functions. Moreover, the number of terms required to represent the experimental problem is difficult to establish a priori, thus a way of proceeding could be increasing the number of terms until no change (within a range) on the result was observed.

In order to solve the equations representing the diffusion problem, the spreadsheet Microsoft Excel 5·0™ (Microsoft Corporation, 1992) was used and non-integer order Bessel functions were included as macros as well as the Legendre polynomials.

To identify the values of D_{eff}, experiments on the drying of potato hemispheres were used. For this purpose, from the spreadsheet containing the experimental data of average dimensionless moisture content versus drying time, the diffusivity coefficient was determined using SOLVER, a tool included in EXCEL that uses an optimization method (Newton or conjugate gradient) to identify one unknown variable by minimizing a criterion.

When using SOLVER, the problem to be addressed must be set up by identifying:

(1) the objective cell, in this case, the objective was to minimize the total sum of squared deviations between the experimental and calculated dimensionless average concentrations;
(2) the changing cells, in this problem, the cell containing the diffusivity value; and
(3) the constraints which the solution must comply with, for the case under consideration, $D_{\mathrm{eff}} > 0$.

The solution of equations representative of mass transfer in hemispherical shaped bodies is more complex than those obtained for other regular geometries (sphere, infinite slab and infinite cylinder). Nevertheless, it is important to consider that by using readily available computing tools this task can be accomplished without a great effort.

To test the advantage of considering the real shape, the results obtained by using hemispherical shape equations were compared to those reached by considering a sphere.

Assuming that both sample size and geometry remain constant, the solution for a sphere in terms of infinite series is known to be [eqn (16)] (Rovedo *et al.*, 1993):

$$\Psi_{\mathrm{M}} = \frac{6}{\mathrm{R}^2\pi^2} \sum_{n=1}^{\infty} \frac{1}{n^2} \exp\left(-\frac{n^2\pi^2 D_{\mathrm{eff}} t}{\mathrm{R}^2}\right) \tag{16}$$

In order to use this equation under the same conditions as the equation for the hemisphere, as an approximate solution the same number of terms of the solution in series was taken into account.

The temperature dependence of the water diffusion coefficient can generally be described by the Arrhenius equation [eqn (17)] (Sarker *et al.*, 1994; Ben Mabrouk & Belghith, 1995).

$$D_{\mathrm{eff}} = D_o \exp\left(- \frac{E_a}{R(T+273)} \right) \tag{17}$$

From this equation, the activation energy can be computed.

In order to evaluate the accuracy of the drying curves simulation obtained by using the models proposed for the two geometries, hemisphere and sphere, the percentage of explained variance (%var) [eqn (18)] was calculated by comparison of computed with experimental moisture content values.

$$\%\mathrm{var} = \left[1 - \left(\frac{S_{yx}^2}{S_y^2} \right)\right]^{\frac{1}{2}} \times 100 \tag{18}$$

MATERIALS AND METHODS

Potatoes (cv. *Claustar*), provided by a local grower were the raw material used in all experiments. Before drying, potatoes were peeled, cut into hemispheres and blanched for 3 min by steam (Rosselló *et al.*, 1992).

The drier used for sample dehydration, described previously by Simal *et al.* (1996a), was equipped with four 500 W electric resistances (at 380 V) coupled to an automatic temperature controller linked to a PC Vectra QS/20 HP. A 0·5-C.V fan impelled the air through the drying bed. A load density corresponding to a monolayer (3·4 kg m^{-2}) was used in order to allow mass transfer through the whole solid surface. The weighing was automatically performed with a Mettler (Switzerland) PM2000 balance linked to the computer ($\pm$0·01 g). The sampling frequency was set-up in order to assume that at least 1% weight change was detected or 0·15 g, this implies that sampling frequency change along the experiment. For weighing purposes, a three-way pneumatic valve deviated the air stream. Temperature control, data acquisition and storage, as well as the general supervision of the unit, start-up and shut down, were all done by the computer program.

Three sets of drying experiments were carried out by using different air drying temperatures and sample sizes (Table 1). The air velocity was > 3 m s^{-1} in order to ensure that internal resistance prevails.

Set a

Experiments performed at different air drying temperatures (30, 50, 70 and 90°C) with hemispheres of $1{\cdot}28 \times 10^{-2}$ m of radius.

Set b

Experiments performed at different air drying temperatures (40, 45, 60, 65, 80 and 85°C) with hemispheres of $1{\cdot}28 \times 10^{-2}$ m of radius.

Set c

Experiments performed at three different air drying temperatures, 45, 65 and 85°C, with hemispheres of $1{\cdot}60 \times 10^{-2}$ m of radius and another at 65°C with hemispheres of $2{\cdot}30 \times 10^{-2}$ m of radius.

The average air flow rate ($2{\cdot}5$ m s^{-1}) was high enough to ensure that drying was mainly controlled by the internal resistance to mass transfer (Rosselló *et al.*, 1992).

TABLE 1
Experimental Conditions of Air Drying Temperature and Hemisphere Radii Corresponding to the Three Sets of Experiments and Percentages of Explained Variance through Proposed Model for Hemispherical and Spherical Shapes

T *(°C)*	*R (10²)(m)*	*%var*	
		Hemispherical model	*Spherical model*
Set a			
30	1·28	99·8	96·7
50	1·28	99·7	96·8
70	1·28	99·9	97·8
90	1·28	99·9	99·1
Average %var =		99·8 ± 0·1	97·6 ± 1·1
Set b			
40	1·28	99·8	96·6
45	1·28	99·4	96·2
60	1·28	99·7	97·1
65	1·28	99·8	96·7
80	1·28	99·9	96·5
85	1·28	99·6	98·0
Average %var =		99·7 ± 0·2	96·9 ± 0·6
Set c			
45	1·60	99·4	96·0
65	1·60	99·7	95·7
65	2·30	99·7	95·5
85	1·60	99·4	94·2
Average %var =		99·6 ± 0·2	95·4 ± 0·8

The average room air characteristics were 21 ± 1°C and 41 ± 8% humidity. The moisture content of the dried product was obtained in triplicate (measure deviation: ±0·2%) according to the AOAC method No. 934.06 (AOAC, 1990).

RESULTS AND DISCUSSION

Experiments of set a were used to identify the model parameters whereas experiments of sets b and c were used to evaluate the accuracy of the model in the simulation of the experiments not involved in parametric identification. For most of the drying period considered the hemispherical shape was fairly well maintained and only at low moisture contents the potato bends and exhibit a non-uniform shrinkage.

Drying curves

Drying kinetics were studied for average moisture contents from 5·1 to 0·2 kg water per kg dm. Induction periods or constant rate periods were not observed. Only one falling drying rate period was observed in the drying curves of potato hemispheres at the different air drying temperatures used, from 30 to 90°C. In Fig. 2, as an example, the drying curves of potato hemispheres have been represented for three

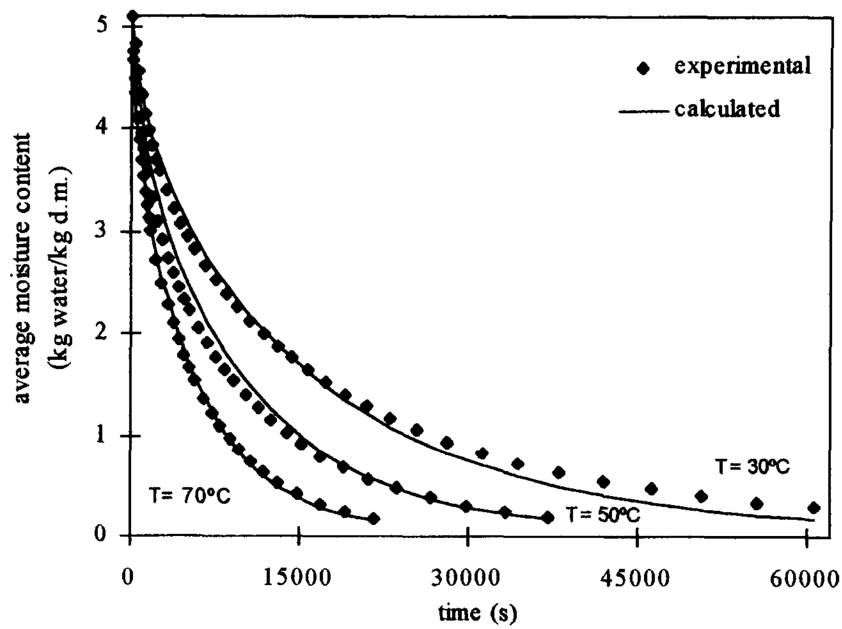

Fig. 2. Experimental and calculated average moisture content versus drying time. Calculated values were determined assuming a hemispherical shape. $R = 1{\cdot}28 \times 10^{-2}$ m.

different drying air temperatures (30, 50 and 70°C). These curves of dehydration showed an important increase in drying rates when increasing air temperature. Similar results were found by different authors (Medeiros & Sereno, 1994; Simal *et al.*, 1996b).

The average moisture content was converted to average dimensionless moisture content (Ψ_M). Taking into account that no constant rate period was observed, the critical moisture content, W_c, was considered to be equal to the initial moisture content, W_0. The equilibrium moisture content, W_e, was determined by using both the room air conditions and the moisture isotherm proposed by Sánchez *et al.* (1997) for potato.

Proposed diffusional model for hemispherical shape

Using the proposed model, the effective diffusivity was identified at four different temperatures (30, 50, 70 and 90°C). It was found that considering only one term for n, on the one hand, and five for m, on the other hand, in eqn (14) was sufficient, more terms did not bring an improvement according to the accuracy of the experiments. The identified diffusivity values, which varied considerably with air drying temperature (from $2{\cdot}7\times10^{-10}$ m^2 s^{-1} at 30°C to $10{\cdot}2\times10^{-10}$ m^2 s^{-1} at 90°C), agree well with the literature data regarding potato diffusion: 8×10^{-10} m^2 s^{-1} at 60°C in slabs (Mohr, 1994); $3{\cdot}8\times10^{-10}$ m^2 s^{-1} at 60°C in cubes (Simal *et al.*, 1994) among others. These identified values were fitted to the Arrhenius equation [eqn (17)]. The results of the fitting can be seen in Fig. 3 and are reported in:

$$D_{\text{eff}} = 8{\cdot}04\times10^{-7}\exp\left(-\frac{20034.6}{R(T+273)}\right) \tag{19}$$

where $r^2 = 0{\cdot}991$.

From this expression, the activation energy for the diffusional process can be estimated. This value, 20·0 kJ mol^{-1}, is similar to those proposed by different authors for potato drying: 27·8 kJ mol^{-1} in *Bintje* potato slabs (Yusheng & Poulsen, 1988); 19·2 kJ mol^{-1} in *Claustar* potato cubes (Rosselló *et al.*, 1992).

Eqn (19) and the proposed model were used to simulate the drying curves of experiments of set a (Table 1). Calculated moisture contents for drying curves at 30, 50 and 70°C were also represented versus drying time in Fig. 2. Percentage of variance explained in the simulation of experiments of set a are shown in Table 1. Average %var was $99{\cdot}8\pm0{\cdot}1$. As it can be seen in Fig. 2 and Table 1, through the proposed model, drying curves of potato hemispheres were accurately simulated.

Evaluation of proposed model

The proposed model was further tested by evaluating drying kinetic simulation of experiments of sets b and c, carried out at both air temperatures and particle sizes not used in the effective diffusivity identification. In Table 1, percentages of explained variance obtained in the simulation of these experiments are shown. The high average %var indicates that the simulation was satisfactory. Moreover, it can be observed that simulation was accurate not only for experiments carried out at

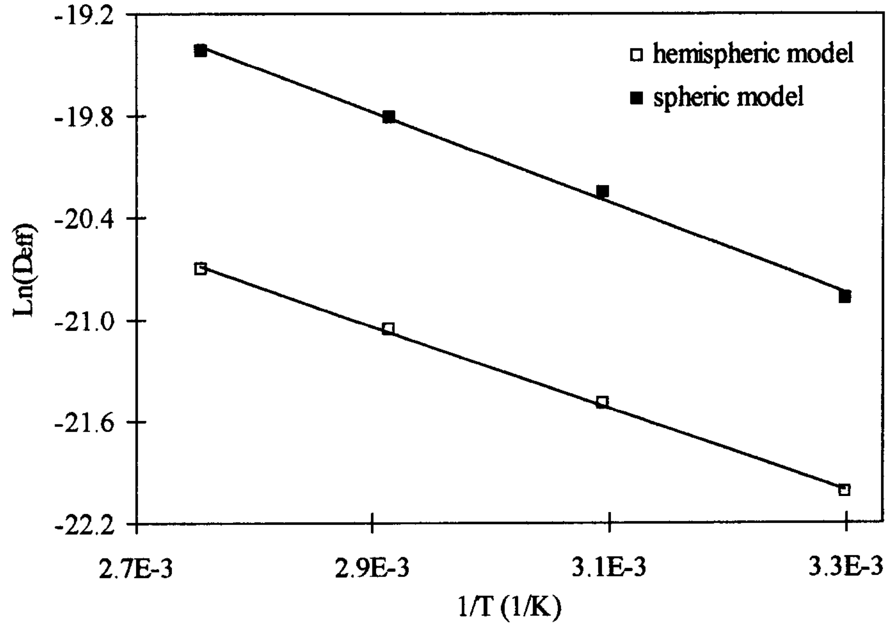

Fig. 3. Influence of temperature on the effective diffusivity coefficient identified assuming a hemispheric or spheric shape.

different air drying temperatures (average %var was $99{\cdot}7 \pm 0{\cdot}2$) but also when air temperature and sample size were modified (average %var was $99{\cdot}6 \pm 0{\cdot}2$).

In Fig. 4, calculated dimensionless moisture at different air drying temperatures (45, 65 and 85°C) and with hemispheres of different size than that used in the experiments for the identification, with radius of $1{\cdot}60 \times 10^{-2}$ m (experiments of set c), has been represented versus the experimental dimensionless moisture. In this figure, the same behavior than that observed in Fig. 2 is shown. Thus, using the proposed model it was possible to simulate the drying curves of potato hemispheres at different experimental conditions of air drying temperature and sample sizes. Although the results are satisfactory in Fig. 4 it is observed that at low moisture contents there is a systematic deviation thus revealing an influence of moisture content on the effective diffusivity (Karathanos *et al.*, 1995).

Diffusional model for spherical shape

Although the results attained using the proposed model were accurate, the importance of taking into account the solid shape when establishing a simple diffusional model to simulate the drying curves was evaluated. Experimental curves of dehydration of potato hemispheres at 30, 50, 70 and 90°C were used to identify the effective diffusivity coefficient using the well known mass transfer equations corresponding to the spherical geometry.

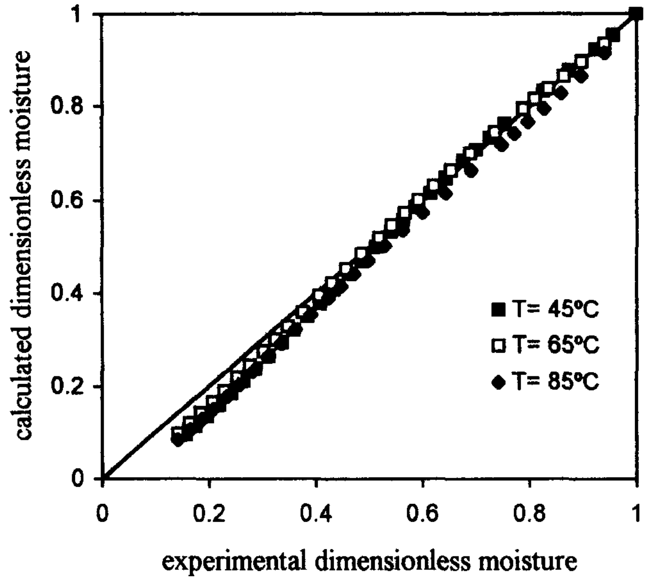

Fig. 4. Comparison of the experimental dimensionless moisture contents with those obtained using the proposed model for hemispherical shape. Data have not been used for effective diffusivity identification. R = $1{\cdot}60 \times 10^{-2}$ m.

The identified diffusional coefficients are shown in Fig. 3. They were fitted to the Arrhenius equation [eqn (17)] and the following expression was obtained:

$$D_{eff} = 9{\cdot}07 \times 10^{-6} \exp\left(- \frac{20098.0}{R(T+273)} \right) \tag{20}$$

where $r^2 = 0{\cdot}997$.

From this equation, the activation energy calculated assuming a spherical geometry was $22{\cdot}1 \text{ kJ mol}^{-1}$, slightly higher than the figure calculated for the hemispherical geometry. As it can be seen, the activation energy is well approached regardless of the model as shown by Mulet (1994). The diffusion coefficient varies from $1{\cdot}4 \times 10^{-9} \text{ m}^2 \text{ s}^{-1}$ at 30°C to $6{\cdot}0 \times 10^{-9} \text{ m}^2 \text{ s}^{-1}$ at 90°C, figures considerably higher than those calculated for hemispheres.

Using eqn (20), moisture contents corresponding to experiments of set a were calculated. The percentage of variance explained in the simulation of these experiments are shown in Table 1. Average %var was $97{\cdot}6 \pm 1{\cdot}1\%$. As it can be observed through these results, the accuracy of the simulation attained with the spherical model was substantially worse than that obtained assuming the actual hemispherical shape.

Calculated dimensionless moisture contents through the proposed model for hemispherical and spherical shapes have been represented in Fig. 5 versus drying time for the experiment of set c carried out at 65°C and with hemispheres of $2{\cdot}30 \times 10^{-2}$ m of radius. In this figure, it can be seen that simulation provided by the proposed model when the real solid shape was considered was accurate whereas calculated results were very different from those experimental when a different shape was considered.

These results are indicative of the importance of taking into account the real shape of the solid being dehydrated when modelling.

Conclusions

Mass transfer equations in an unsteady boundary problem have been solved for hemispherical solids through the separation of variables method. The drying curves of hemispherical potatoes have been adequately simulated at different drying air temperatures (from 30 to 90°C) by using this simple method (average %var = 99·7%). The importance of taking into account the real geometry of the solid was evaluated by using the solution for a spherical shaped body. The model developed for a sphere provided less satisfactory results in the simulation of the drying experiments of hemispherical potato samples (average %var = 96·6%).

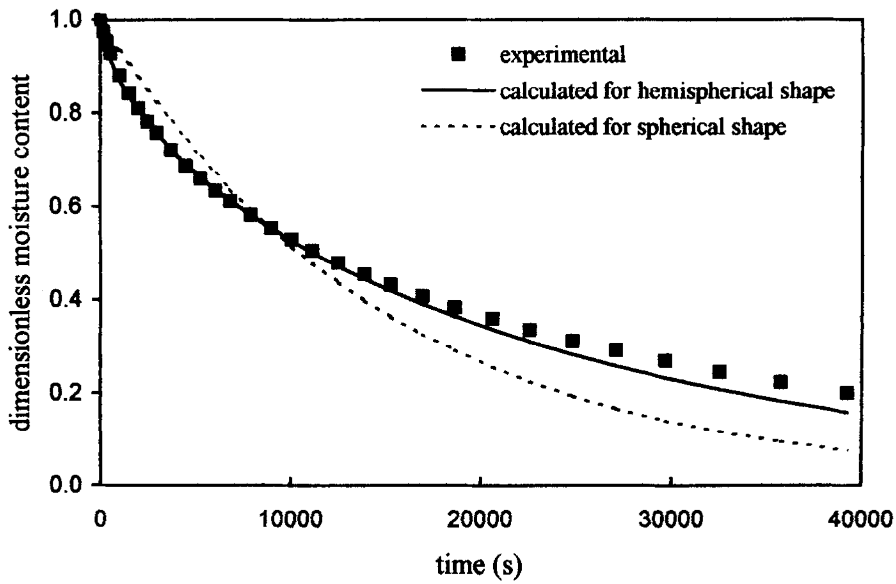

Fig. 5. Experimental and computed dimensionless moisture content obtained using the proposed diffusional models for hemispheric and spheric shapes vs drying time. Data have not been used for effective diffusivity identification. $R = 2{\cdot}30 \times 10^{-2}$ m.

ACKNOWLEDGEMENTS

The authors acknowledge the financial support of CICYT (ALI94-0565-C03) and M. Forcén for her suggestions on the English language editing.

REFERENCES

Aminabhavi, T. M. & Phyade, H. T. S. (1995). Solvent migration and drying phenomenon of polymeric blends of ethylene-propylene random copolymer and isotactic polypropylene in the presence of monocyclic aromatic liquids at temperatures between 25–70°C. *Drying Technol.*, **13**(8 and 9), 1841–1879.

AOAC (1990). Official method of analysis of the Association of Official Analytical Chemist. No. 934.06. AOAC, Arlington, VA, USA.

Arpaci, V. S. (1966). *Conduction Heat Transfer*. Addison–Wesley, Reading, MA, USA.

Ben Mabrouk, S. & Belghith, A. (1995). Numerical simulation of the drying of a deformable material: evaluation of the diffusion coefficient. *Drying Technol.*, **13**(8 and 9), 1789–1805.

Dincer, I. & Dost, S. (1995). An analytical model for moisture diffusion in solid objects during drying. *Drying Technol.*, **13**(1 and 2), 425–435.

Fusco, A. J., Avanza, J. R., Aguerre, R. J. & Gabitto, J. F. (1991). A diffusional model for drying with volume change. *Drying Technol.*, **9**(2), 397–417.

García-Reverter, J., Berna, A., Chinesta, F., Girona, M. A. & Mulet, A. (1996). Drying kinetics of cauliflower florets. In *Drying '96*, vol. B, eds. Strumillo C. & Pakowski Z. Lodz Technical University, Lodz, Poland, pp. 913–920.

Jaros, M., Cenkowski, S., Jayas, D. S. & Pabis, S. (1992). A method of determination of the diffusion coefficient based on kernel moisture content and its temperature. *Drying Technol.*, **10**(1), 213–222.

Karathanos, V. T., Villalobos, G. & Saravacos, G. D. (1990). Comparison of two methods of estimation of the effective moisture diffusivity from drying data. *J. Food Sci.*, **55**(1), 218–231.

Karathanos, V. T., Kostaropoulos, A. E. & Saravacos, G. D. (1995). Air-drying of osmotically dehydrated fruits. *Drying Technol.*, **13**(5–7), 1503–1521.

Medeiros, G. L. & Sereno, A. M. (1994). Physical and transport properties of peas during warm air drying. *J. Food Engng*, **21**, 355–363.

Microsoft Corporation (1992). *Spreadsheet User's Manual*, EXCEL 5·0, Redmon, WA, USA.

Mohr, K. H. (1994). Kinetics of moisture transport in biological products under drying conditions. *Int. Chem. Engng*, **34**(2), 210–212.

Mulet, A. (1994). Drying modelling and water diffusivity in carrots and potatoes. *J. Food Engng*, **22**, 329–348.

Rosselló, C., Cañellas, J., Simal, S. & Berna, A. (1992). Simple mathematical model to predict the drying rates of potatoes. *J. Agric. Food Chem.*, **40**, 2374–2378.

Rovedo, C. O., Aguerre, R. J. & Suarez, C. (1993). Moisture diffusivities of sunflower seed components. *Int. J. Food Sci.Technol.*, **28**, 159–168.

Sánchez, E. S., SanJuan, N., Simal, S. & Rosselló, C. (1997). Calorimetric techniques applied to the determination of isosteric heat of desorption for potato. *J. Sci. Food Agric.*, **74**, 57–63.

Sarker, N. N., Kunze, O. R. & Strouboulis, T. (1994). Finite element simulation of rough rice drying. *Drying Technol.*, **12**(4), 761–775.

Simal, S., Berna, A., Mulet, A. & Rosselló, C. (1994). Heat and mass transfer model for potato drying. *Chem. Engng Sci.*, **49**(22), 3739–3744.

Simal, S., Mulet, A., Catalá, P. J., Cañellas, J. & Rosselló, C. (1996). Moving boundary model for simulating moisture movement in grapes. *J. Food Sci.*, **61**(1), 157–160.

Simal, S., Mulet, A., Tarrazó, J. & Rosselló, C. (1996). Drying models for green peas. *Food Chem.*, **55**(2), 121–128.
Tolaba, M. P., Aguerre, R. J. & Suarez, C. (1989). Shape characterization for diffusion analysis of corn drying. *Drying Technol.*, **7**(2), 205–217.
Vanegas, G. K. & Marinos-Kouris, D. (1991). Drying kinetics of apricots. *Drying Technol.*, **9**(3), 735–752.
Waananen, K. M., Lichfield, J. B. & Okos, M. R. (1993). Classification of drying model for porous solids. *Drying Technol.*, **11**(1), 1–40.
Yusheng, Z. & Poulsen, K. P. (1988). Diffusion in potato drying. *J. Food Engng*, **7**, 249–262.
Zakhia, N., Bohuon, P. & Collignan, A. (1995). Modelling of fish drying kinetics using a combination of surface response methodology and diffusional models. *Drying Technol.*, **13**(8 and 9), 2083–2096.
Zogzas, N. P., Maroulis, Z. B. & Marinos-Kouris, D. (1994). Moisture diffusivity. Methods of determination. A review. *Drying Technol.*, **12**(3), 483–515.